JOURNAL OF MATERIALS SCIENCE 12 (1977) 2456–2464

Steady-state creep of an alloy based on the intermetallic compound $Ni_3Al(\gamma')$

J. R. NICHOLLS*, REES D. RAWLINGS
Department of Metallurgy and Materials Science, Imperial College, London, UK

An investigation of the steady-state creep of a Ni_3Al.10 at % Fe alloy (γ') has shown that two creep mechanisms were operative over the temperature range 530 to 930° C. The experimental data at low temperatures (below 680° C) were not consistent with any of the established creep theories. However, the experimental data were in good agreement with a proposed model for cross-slip from octahedral {1 1 1} planes on to cube {1 0 0} planes in LI_2 crystals. Above 680° C, the rate-controlling mechanism, which had an activation energy of 3.27 eV $atom^{-1}$, is considered to be the removal/production of APBs during climb.

1. Introduction

In the majority of nickel-base superalloys the strength at elevated temperatures is attributed in the main to the presence of a dispersion of the intermetallic compound Ni_3Al (γ'). γ' can accommodate considerable quantities of alloying elements in solution and analysis has shown that γ'-precipitates in superalloys contain various elements such as titanium, chromium and niobium. In view of the role played by γ' in these alloys, and the quest for materials to operate at higher temperatures it is appropriate to investigate the creep behaviour of γ' and its alloys.

Sherby and Burke [1], or reviewing the creep behaviour of metals and alloys, concluded that the steady-state creep rate $\dot{\epsilon}$ of most fine-grained polycrystalline metals, non-metals and solid solutions, at temperatures above half their melting point T_m, is controlled by the rate of atom mobility. Below half the melting point, extensive recovery can no longer take place by atomic diffusion and other thermally activated processes are rate-controlling. Typical examples of rate-controlling creep mechanisms for both diffusion and non-diffusion controlled processes are tabulated in Table I.

Although the creep properties of nickel-base superalloys are well documented there is little information available on the creep of γ' and its alloys. Thornton *et al.* [2] have studied transient creep in γ' contianing 2% Cr and observed two creep mechanisms over the temperature range 25 to 626° C. At the lower temperatures, and at low stresses at intermediate temperatures, the transient creep response indicated an exhaustion of the mobile dislocation density. In contrast at the higher temperature, and at high stresses at intermediate temperatures, recovery effects were rate-controlling.

To the author's knowledge, the only published work on steady-state creep in alloys based on Ni_3Al is that by Flinn [3] on γ' containing 10% iron. This work showed that creep over the temperature range 816 to 1093° C (0.65 to 0.82 T_m) was diffusion controlled. Flinn proposed that the rate-controlling process was the diffusion of atoms to and from the antiphase domain boundaries (APBs). Under these conditions the creep rate will depend on the rate of formation of wrong bonds in front of a leading superpartial dislocation and hence depends on the net jump rate of atoms in the direction of the applied stress. Flinn concluded that Weertman's [11] analysis for microcreep should be applicable and successfully fitted his experimental data to the appropriate equation (see Table I).

This paper reports the results of an investigation of the steady-state creep chracteristics of an alloy of similar composition to that studied by Flinn.

*Presently at Department of Materials, Cranfield Institute of Technology, Cranfield, Bedford.

TABLE I Proposed rate-controlling creep mechanisms

Mechanism	Theoretical equations*	References
Non diffusion controlled mechanisms		
Movement of dislocations over Peierls barriers	$\dot{\epsilon} = C \exp\left[\frac{-\Delta H_0(1+\phi_p)}{kT}\right] . \exp\left[B(\sigma - \sigma_\mu)\right]$	Conrad [4]
	where $\phi_p = \frac{1}{4}\log\left[\frac{16\sigma_p}{\pi\sigma}\right]$; ΔH_0 = Kink energy;	Weertman [5]
	σ_p = Peierls stress.	
Intersection of dislocations	$\dot{\epsilon} = C \exp -\left[\frac{\Delta H_0 - V^*(\sigma - \sigma_\mu)}{kT}\right]$	Seeger [6]
	where ΔH_0 = intersection energy;	
	V^* = activation volume	
Cross-slip	$\dot{\epsilon} = C \exp -\left[\frac{\Delta H_0 - c \ln(\sigma/\sigma_c)}{kT}\right]$	Schoeck and Seeger [7]
	where ΔH_0 = energy for cross slip;	
	σ_c = critical resolved shear stress	
Diffusion controlled mechanisms		
Movement of jogged screw dislocations	$\dot{\epsilon} = C \exp\left[\frac{-\Delta H_{SD}}{kT}\right] \sinh\left[\frac{1b\sigma^2}{kT}\right]$	Mott [8]
	where ΔH_{SD} = activation energy for self-diffusion:	
	1 = spacing of jogs; b = Burgers vector	
Climb of edge dislocations	$\dot{\epsilon} = C\sigma^n \exp\left[\frac{-\Delta H_{SD}}{kT}\right] \sinh\left[\frac{B\sigma^m}{kT}\right]$	Weertman [9] Weertman [10]
	where $m \sim n \sim 2$; ΔH_{SD} = activation energy of self-diffusion.	
Drag of solute atoms (Viscous type dislocations motion)	$\dot{\epsilon} = C\sigma^n \exp\left[\frac{-\Delta H_{SD}}{kT}\right]$	Weertman [11] Cottrell [12]
	where $n = 1$ or 3; ΔH_{SD} = activation energy of self-diffusion.	
Diffusion creep	$\dot{\epsilon} = \frac{10\sigma d^3 D}{L^2 kT}$ (Nabarro–Herring Equation)	Nabarro [13] Herring [14] Williams [15]
	$\dot{\epsilon} = \frac{B\sigma d D}{L^2 kT}$ (Coble Equation-Grain boundary diffusion creep)	Coble [16]
	where D = diffusion coefficient; L = grain diameter;	
	d = atom diameter.	

*Symbols: $\dot{\epsilon}$ = strain-rate; σ = applied stress; σ_μ = internal stress; T = temperature; k = Boltzmann's constant; B, C and c are constants; ΔH = activation energy.

However, the range of testing temperatures (580 to 960° C) employed in the present investigation is extended to lower temperatures than those used by Flinn.

2. Experimental procedure

The alloy (nominally Ni_3Al.10 at % Fe) was supplied by the International Nickel Company in the form of a vacuum-cast ingot of approximately 2 kg. Smaller ingots were prepared by melting 50 g charges of this alloy in an electric-arc furnace. Following casting, all ingots were homogenized at 1000° C for 24 h and then quenched into iced water. Light and electron microscopy confirmed that the alloy was single phase after the homogenization treatment and also after creep testing.

A typical analysis for the three major constituents, plus the trace elements copper and silicon (possible contaminants from the arc casting and subsequent heat-treatment), of an homogenized arc-cast ingot is presented in Table II. The alloy is not-stoichiometric (aluminium-rich) assuming that iron substitutes equally for nickel and aluminium once a critical concentration (~1.0 at. %) of iron on the aluminium sublattice has been exceeded [17].

Difficulties associated with the fabrication of tensile creep specimens were alleviated by testing in uniaxial compression. Specimens 5 mm x

TABLE II Analysis of an homogenised arc-cast ingot

Element	(wt%)	(at.%)
Ni	77.00	68.23
Al	10.94	21.09
Fe	11.46	10.68
Cu	<100 ppm	–
Si	<100 ppm	–

2 mm x 2 mm were cut from the homogenized ingots, using a fine silicon carbide slit grinding wheel, and then polished on all faces. The creep tests were carried out in a constant load machine with extensometry capable of detecting creep rates of $5 \times 10^{-9}\,\mathrm{sec}^{-1}$. Specimens were tested over the temperature range 530 to 930° C with stresses varying from 100 to 600 $\mathrm{MN\,m}^{-2}$. Temperature and load cycling tests were used to determine the temperature and stress dependence of the steady-state creep rate at constant structure. A more detailed account of the experimental procedure is given in [18].

3. Results

The steady-state creep data for Ni_3Al.10 at.% Fe are presented in Figs. 1–3. Fig. 1, which is a conventional Arrhenius plot, summarizes the temperature dependence of the steady-state creep rate at constant stress. This plot indicates that there are two creep mechanisms operating over the temperature range of the investigation. The lower temperature mechanism is characterized by a smaller gradient and the transition from one mechanism to another is around 650 to 700° C. It is well established that the flow stress of γ' and its alloys increases with increasing temperature, reaching a peak value at a temperature, T_p, which depends on the degree of stoichiometry and alloying addition [19]. It is of interest to note that the peak temperature of the alloy used in the present investigation was approximately 700° C [18], i.e. in the same temperature range as the proposed changes in creep mechanisms.

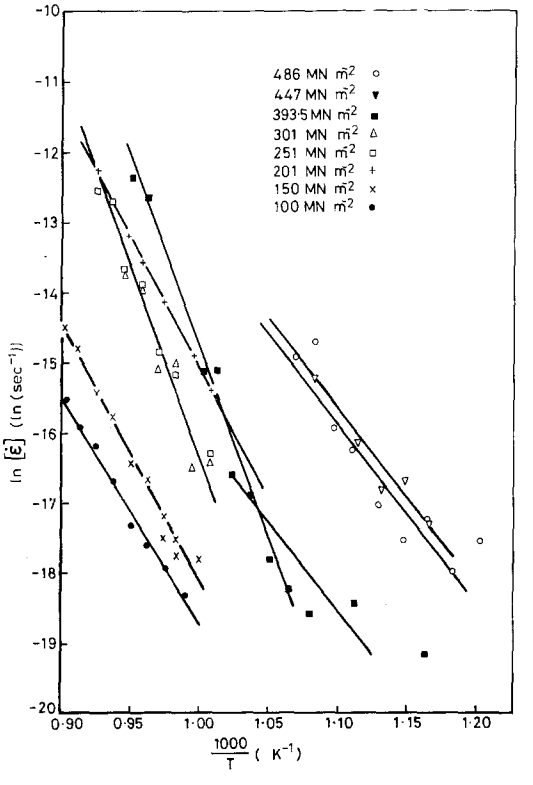

Figure 1 The temperature dependence of the steady-state creep rate in Ni_3Al.10 at.% Fe.

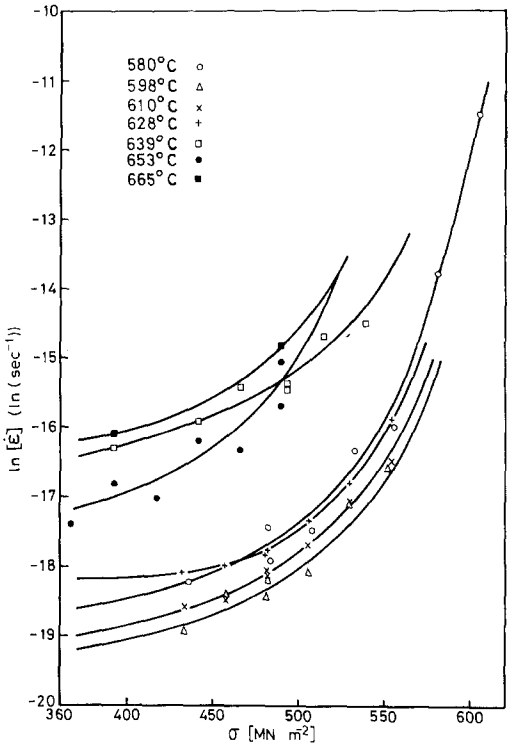

Figure 2 Plot showing that the stress dependence of the steady-state creep rate is not exponential at temperatures below 680° C.

Accepted rate-controlling mechanisms (Table I) require that either the creep rate depends exponentially on stress [4–6] or that it exhibits a power law dependence [8–16]. As can be seen from the load cycling data for temperatures below 680° C, neither an exponential nor a power law stress dependence is observed (Figs. 2 and 3). Thus, current creep theories do not satisfactorily describe

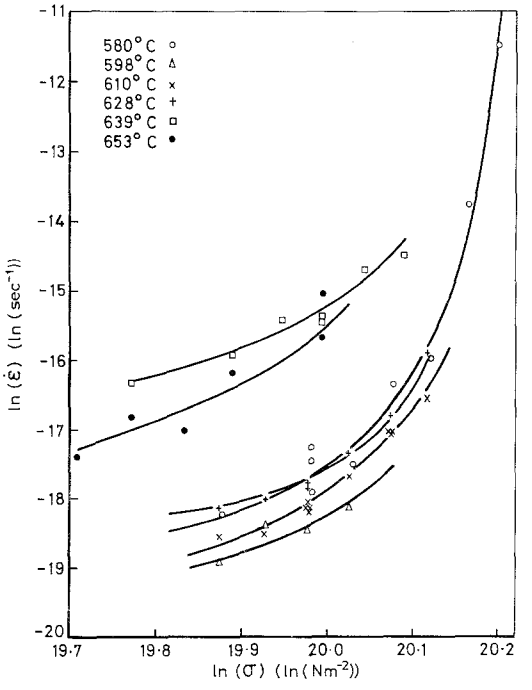

Figure 3 Graph showing that there is not a power law dependence of the steady-state creep rate on stress.

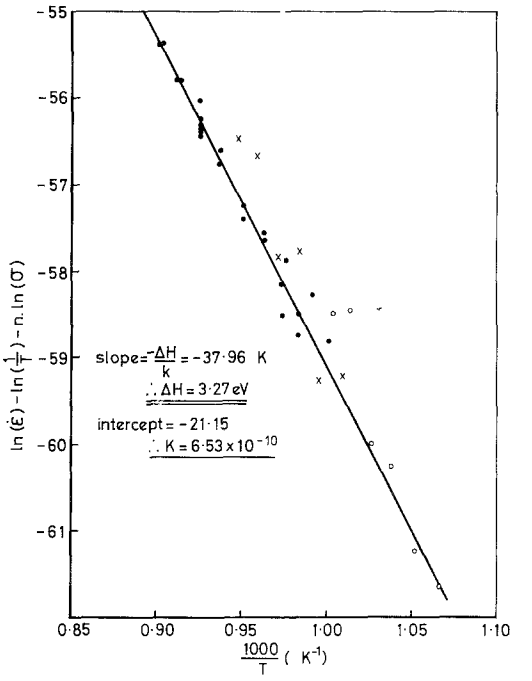

Figure 4 Plot to determine the activation energy for creep in the temperature range 680 to 930° C using Equation 1.

the creep behaviour of γ' at these low temperatures.

4. Discussion

4.1. Steady-state creep in the temperature range 680 to 930° C

An electron microscopy study of Ni_3Al.5.5 at. % Ti has shown that, at tempeatures in excess of 550° C (T_p for the alloy), the dislocation structure consists of predominately edge dislocation dipoles which show a tendency to collapse to form rows of loops [20]. The collapse of the edge dipoles occurs by dislocation climb and the removal/production of APBs by diffusion.

If it is assumed that the dislocation structure is common to all γ' alloys at temperature above T_p, and that the collapse of the dipoles is the rate-controlling creep mechanism, then an argument closely following that of Flinn's [3] may be applied. Flinn proposed that the creep of Ni_3Al.10 at. % Fe at temperature above 800° C is governed by the rate of motion of sections of dislocation loops which are not in the slip plane. Hence the rate-controlling step is the removal/production of APBs by thermal motion of neighbouring atoms. Such dislocation motion is a viscous drag mechanism and consequently Weertman's analysis of microcreep should apply [11]:

$$\dot{\epsilon} = \frac{K}{T}\sigma^n \exp\left[-\frac{\Delta H}{KT}\right] \qquad (1)$$

where $K = \dfrac{2\pi D_0 b}{Gk}$. D_0, b, G and k are the diffusion coefficient, the Burgers vector, the shear modulus and Boltzmann's constant respectively. n is a constant which is equal to three.

The high temperature (>680° C) creep data obtained in the present investigation are plotted, according to Equation 1, in Figs. 4 and 5. The values determine for K, n and ΔH from these graphs are given in Table III.

In applying Weertman's analysis of microcreep to the high temperature creep deformation in γ', Flinn suggested that ΔH consisted for two components, namely an energy for self-diffusion

TABLE III Constants in Equation 1, determined by applying Weertman's microcreep analysis [11] to high temperature creep deformation in Ni_3Al.10 at. % Fe.

	K $(N m^{-2})^{-n}$	n	ΔH (eV atom^{-1})
Present work	$10^{-9.2 \pm 1.5}$	2.56 ± 0.24	3.27 ± 0.30
Flinn [3]	$10^{-13.8 \pm 1.4}$	3.2 ± 0.2	3.38 ± 0.09
Calculated from theory	$10^{-11.16}$	3	3.55

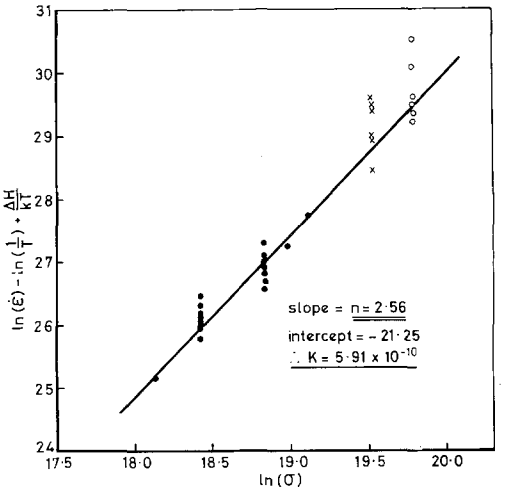

Figure 5 Plot to determine the stress exponent n for creep in the temperature range 680 to 930° C using Equation 1.

ΔH_{SD}, and an energy, η, necessary to produce wrong bonds:

$$\Delta H = \Delta H_{SD} + \eta \quad (2)$$

Theoretical values for ΔH and K were calculated from Equations 1 and 2 using the following values of the constants for Ni_3Al: $G = 5.7 \times 10^{10}$ N m^{-2} [21], $b = 5.03 \times 10^{-10}$ m [18], $\Delta H_{SD} = 3.14$ eV atom^{-1} [22], $D_0 = 10^{-4}$ m^2 sec^{-1} [22] and $\eta = 0.41$ eV atom^{-1} [3].

As shown in Table III, good agreement was obtained between the theoretical and experimental values (all the experimental values lie within 95% confidence limits of their respective theoretical values). The experimental activation energy for creep (3.27 eV atom^{-1}) is slightly lower than the calculated value of 3.55 eV atom^{-1}. However, Hancock [22] found that the addition of 5 at.% Ti to Ni_3Al reduced ΔH_{SD} by approximately 0.5 eV atom^{-1}. Hence the experimental value of ΔH for Ni_3Al.10 at.% Fe may be lower than the theoretical value for Ni_3Al because the iron solute lowers ΔH_{SD}.

Finally, the present results closely agree with those determined by Flinn over the temperature range 800 to 1180° C, indicating that the same mechanism is operative from 680 to 1180° C.

4.2. Steady-state creep at temperatures below 680° C

At temperatures below half the melting point (the melting point, T_m, for Ni_3Al.10 at.% Fe is 1390° C) diffusion-controlled processes are very slow, hence other thermally activated mechanisms must be responsible for creep. Studies of creep in fcc metals at temperatures of less than 0.5 T_m indicate that the rate-controlling mechanism may be cross-slip [7, 23]. Furthermore, an electron microscopy study of Ni_3Al.5.5 at.% Ti has shown that over the temperature range 0.61 to 0.93 T_p (where T_p is the peak temperature) cross-slip readily occurs from octahedral {1 1 1} to cube {1 0 0} and from cube to octahedral planes [20]. Consequently it is proposed that cross-slip is the rate-controlling mechanism for creep in Ni_3Al.10 at.% Fe at temperatures below 680° C, (i.e. over the temperature range of 0.84 to 0.98 T_p).

The available cross-slip mechanisms are not applicable to cross-slip in γ' as they cannot take into account that, (i) γ' has the $L1_2$ structure and hence cross-slip involves stacking fault and APB energies, and (ii) cross-slip to and from octahedral and cube planes must be considered [20, 24]. The following cross-slip mechanism has been developed for $L1_2$ Ni_3Al, but with minor changes could be modified for other ordered structures.

4.2.1. A cross-slip mechanism for Ni_3Al

The various steps in the cross-slip of a superlattice dislocation in the $L1_2$ structure from the primary octahedral plane to an octahedral or cube plane are given in Fig. 6. Firstly, the Shockley partial constricts forming a node in the primary {1 1 1} plane. The energy required for construction is U_C (Fig. 6a). The node then expands producing a segment of undissociated $\frac{a}{2}\langle 1\,1\,0\rangle$ screw dislocation. The energy for expansion is the energy, U_R, needed to recombine the partial dislocations (Fig. 6b). The next step is the movement of a segment of the dislocation on to the cross-slip plane. The line energy of the dislocation is increased by ΔU_L and a new region of antiphase domain boundary is produced (ΔU_{APB}). These energy requirements are reduced by the work done, W_{CS}, and by the resolved stress on the cross-slip plane (Fig. 6c). Finally, if the cross-slip plane is an octahedral plane, the dislocation segment dissociates again into Shockley partials (Fig. 6c). The activation energy for cross-slip, U_{CS}, is therefore given by the following expressions:

(i) cross-slip from a {1 1 1} to {1 0 0} plane

$$U_{CS} = [U_C + U_R]_{111} + [\Delta U_L - W_{CS}]_{100} + [\Delta U_{APB}]_{100} \quad (3)$$

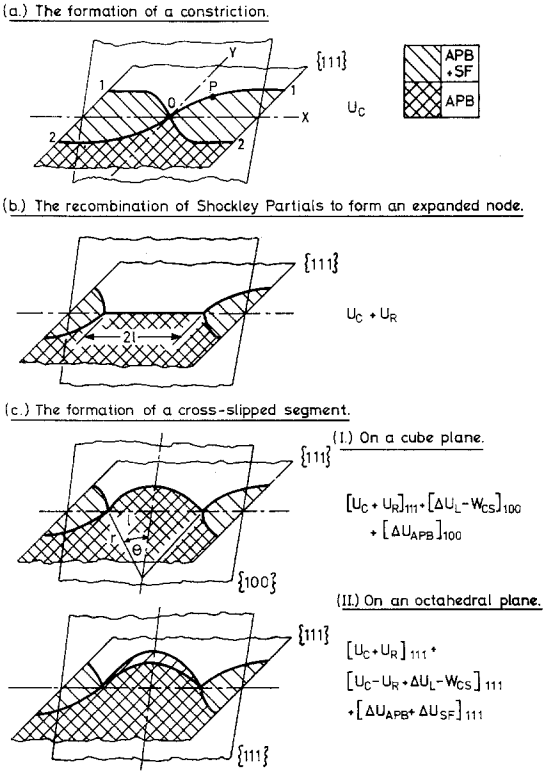

Figure 6 Formation of a cross-slipped dislocation segment.

(ii) cross-slip from a {1 0 0} to {1 1 1} plane

$$U_{CS} = [U_C - U_R + \Delta U_L - W_{CS}]_{111} + [\Delta U_{APB} + \Delta U_{SF}]_{111} \quad (4)$$

(iii) cross-slip from a {1 1 1} to {1 1 1} plane

$$U_{CS} = [U_C + U_R]_{111} + [U_C - U_R + \Delta U_L - W_{CS}]_{111} + [\Delta U_{APB} + \Delta U_{SF}]_{111} \quad (5)$$

In γ', dislocations may cross-slip on to a parallel {1 1 1} plane via a {1 0 0} plane or a {1 1 1} cross-slip plane. Since two alternative routes are available the one with lowest activation energy is likely to occur. Cross-slip via the {1 0 0} plane is accomplished in two steps, namely cross-slip from {1 1 1} to {1 0 0} and then cross-slip from {1 0 0} to {1 1 1}. As these two steps constitute a series process, the step with highest activation energy must be rate-controlling. A comparison of Equations 3 and 4, indicates that cross-slip from {1 1 1} on to a {1 0 0} plane is rate-controlling for cross-slip via a cube plane; $[\Delta U_{APB} + \Delta U_{SF}]_{111} > [\Delta U_{APB}]_{100}$, $[U_C + U_R]_{111} > [U_C - U_R]_{111}$ and $[\Delta U_L - W_{CS}]_{100} \simeq [\Delta U_L - W_{CS}]_{111}$.

By far the most significant contribution to the energy for cross-slip is the constriction energy U_C. Equations 3 and 5 show that the energy for cross-slip from the primary octahedral plane to a {1 0 0} and a {1 1 1} are proportional to U_C and $2U_C$ respectively. Hence the energy required to cross-slip via an octahedral plane is greater than that for a cube plane by a factor of approximately two; this implies that cross-slip from a {1 1 1} on to a {1 0 0} is the rate-controlling step for thermally activated cross-slip in γ'.

The determination of the contributory terms (U_C, U_R, ΔU_L and W_{CS}) to the activation energy for cross-slip are given in Appendix 1. This analysis introduces a new parameter θ, which is the half-angle subtended by the cross-slipped segment of the dislocation (Fig. 6c), into the equation for cross-slip. A stable dislocation loop is formed when θ reaches some critical value θ_c, such that for $\theta > \theta_c$ a decrease in energy occurs as θ increases. The evaluation of θ_c for cross-slip from {1 1 1} onto {1 0 0}, as detailed in Appendix 2, yields the following solutions.

(i) $\cos\theta_c = 1$; hence $\theta_c = 0$, this corresponds to the formation of a stable constriction, with no dislocation loop on the cross-slip plane.

(ii) $$\cos\theta_c = \frac{\gamma_{APB\,100}}{(\tau b)_{100} - \gamma_{APB\,100}}, \quad (6)$$

where τ is the resolved shear stress and γ_{APB} is the antiphase boundary energy on the effective cross-slip plane. For real values of θ_c, $(\tau b)_{100}$ must be greater than $2\gamma_{APB\,100}$. This implies that a critical size of cross-slipped dislocation loop must be formed to be stable. Loops smaller than this critical size will collapse to a stable constriction with $\cos\theta_c = 1$.

The maximum value of U_{CS}, i.e. the activation energy required to form a stable dislocation loop on the cross-slip plane is determined by substituting θ_c, from Equation 6, into Equation 3:

$$U_{CS} = U_{C111} + \frac{\Gamma_{L\,100}^2}{(\tau b)_{100}} \times \left[(1+X)\cos^{-1}\left(\frac{X}{1-X}\right) - \left(\frac{2-X}{1+X}\right)(1-2X)^{1/2}\right] \quad (7)$$

where $X = \gamma_{APB\,100}/(\tau b)_{100}$, Γ is the line tension and $\cos\theta_c = X/(1-X)$ (therefore $0 \leqslant X < \frac{1}{2}$ for real values of θ_c). As X can only take values between 0 and $\frac{1}{2}$, Equation 7 can be expanded using Maclaurin's theorem, giving

$$U_{CS} = U_{C\,111} + \frac{\Gamma^2_{L\,100}}{(\tau b)_{100}} \times \left[\frac{\pi}{4} - 1 + \frac{\pi}{4}X - \frac{X^2}{2} + \frac{\phi X^3}{3}\right] \quad (8)$$

where $\phi = -1.26$ [18]. Defining α as the ratio of $\tau_{111}:\sigma$ and β as the ratio of $\tau_{100}:\sigma$ (where σ is the applied stress), substituting for $U_{C\,111}$, τ_{111} and τ_{100} in Equation 8 and rearranging gives

$$U_{CS} = U_{CO}\left[1 - \frac{\sigma}{A+\sigma}\right] - \frac{B}{\sigma}\left[1 - \frac{\pi}{4} - \frac{\pi}{4}\left(\frac{C}{\sigma}\right) + \frac{1}{2}\left(\frac{C}{\sigma}\right)^2 + 0.42\left(\frac{C}{\sigma}\right)^3\right]$$

where

$$A = \frac{(\gamma_{APB} + \gamma_{SF})_{111}}{\alpha(b_2)_{111}}, \quad B = \frac{2\Gamma^2_{L\,100}}{\beta b_{100}} \quad \text{and}$$

$$C = \frac{\gamma_{APB\,100}}{\beta b_{100}}$$

It can be seen from Fig. 1 that the temperature dependence of the steady-state creep rate at temperatures below 680° C obeys the Arrhenius equation. Therefore, if creep in this temperature range is controlled by cross-slip from {1 1 1} to {1 0 0} planes, the following equation should apply:

$$\ln(\dot{\epsilon}) = -\frac{U_{CO}}{kT}\left[1 - \frac{\sigma}{A+\sigma}\right] + \frac{B}{\sigma kT}\left[1 - \frac{\pi}{4} - \frac{\pi}{4}\frac{C}{\sigma} + \frac{1}{2}\left(\frac{C}{\sigma}\right)^2 + 0.42\left(\frac{C}{\sigma}\right)^3\right] + \ln(K) \quad (9)$$

where K is a constant which depends on the internal structure.

The values for U_{CO}, A, B and K obtained by computer-fitting the data of Figs. 1 to 3, for the temperature range 530 to 680° C, to Equation 9 using an iterative linear least-squares technique are presented in Table IV. A range of values for C were possible, but all were small ($<0.2\,MN\,m^{-2}$) compared with σ and hence all terms containing $\left(\frac{C}{\sigma}\right)$ may be neglected. Thus creep in γ', when controlled by the cross-slip mechanism, obeys the following equation:

$$\dot{\epsilon} = K\exp\left[-\frac{U_{CO}}{kT}\left(1 - \frac{\sigma}{A+\sigma}\right) + \frac{B\left(1-\frac{\pi}{4}\right)}{\sigma kT}\right] \quad (10)$$

This is confirmed in Fig. 7, which shows good agreement between experiment (over a stress range

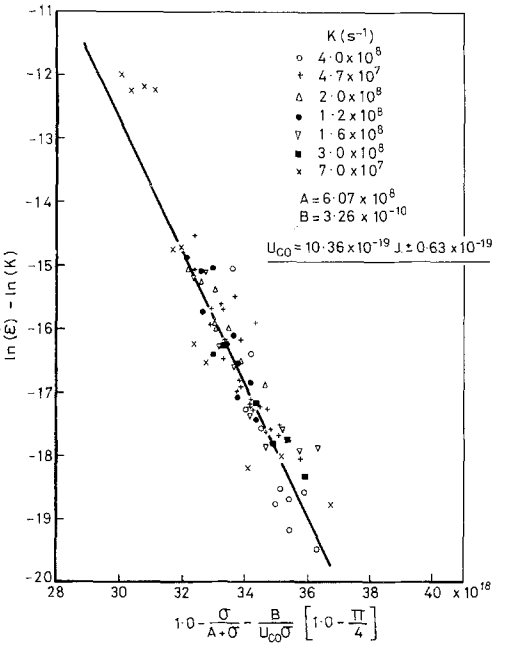

Figure 7 Plot showing that the data below 680° C are in accordance with Equation 10.

TABLE IV Values for the constants in the equation for cross-slip (Equation 9).

Constant	Value	Comment
U_{CO}	6.47 ± 0.40 eV	energy to form a constriction
A	6.07×10^8 J m^{-3}	$= (\gamma_{APB} + \gamma_{SF})_{111}/\alpha(b_2)_{111}$
B	3.26×10^{-10} J^2 m^{-3}	$= 2\Gamma^2_{L\,100}/\beta b_{100}$
$\frac{C}{\sigma}$	typically 5×10^{-4}	may be neglected
K	$0.47 - 4.0 \times 10^8$ sec^{-1}	A range of values (depends on internal structure)

of 360 to 600 MN m^{-2} and temperature range 530 to 680° C) and Equation 10 for creep of Ni_3Al.10 at.% Fe.

5. Conclusions

(1) A model for creep, when controlled by cross-slip from {1 1 1} to {1 0 0} planes, has been developed for Ll_2 crystals. The experimental data for the steady-state creep of Ni_3Al.10 at.% Fe, over the stress range of 360 to 600 MN m^{-2} and the temperature range of 530 to 680° C, were in good agreement with this model.

(2) At more elevated test temperatures (680 to 930° C) the rate-controlling mechanism is considered to be the removal/production of APBs during climb. Weertman's theory of microcreep was found to be applicable with an activation energy for creep of 3.27 eV atom^{-1}.

6. Appendix I

Determination of U_C, U_R, ΔU_L and W_{CS}.

6.1. U_C, the energy to form a constriction

Stroh [25] has shown that the energy to form a constriction, U_C, in an f c c material is a function of the line tension, Γ_L, and separation of the partials, d_{12}, namely

$$U_C = (A\Gamma_L)^{1/2} d_{12} \tag{A1}$$

A is a constant for a given material. Now d_{12} is given by

$$d_{12} = \frac{2-3\nu}{2(1-\nu)} \frac{Ga^2}{24\pi} \frac{1}{\tau_{b2} b_2 + (\gamma_{APB} + \gamma_{SF})} \tag{A2}$$

where ν is Poisson's ratio, γ_{APB} and γ_{SF} are the energies of formation of unit area of APB and stacking fault respectively, τ_{b2} is the local stress parallel to the Burgers vector $\boldsymbol{b}_2$ of the partial. Therefore defining U_{CO} as the constriction energy for zero applied stress one obtains from combining Equations A1 and A2

$$U_C = \frac{U_{CO}(\gamma_{APB} + \gamma_{SF})}{\tau_{b2} b_2 + (\gamma_{APB} + \gamma_{SF})} \tag{A3}$$

for a constriction of the leading partials of an extended superlattice dislocation.

6.2. U_R, the energy to recombine the Shockley partials

If E_R is the recombination energy/unit length of dislocation, then:

$$U_R = E_R 2l \tag{A4}$$

where l is the length of the recombined segment (Fig. 6b).

Dorn [26] has shown that the energy required per unit length to recombine two Shockley partials is,

$$E_R = \int_{d_\tau}^{b} \frac{3}{4} \frac{Ga^2}{24\pi} \frac{-dx}{x} - (\tau_1 b_1 + \gamma_{SF})(d_\tau - b) + (\Lambda - 2\Lambda_p) - b(\tau_1 b_1 + \gamma_{SF})$$

where Λ and Λ_p are the core energies of a unit and a partial dislocation respectively and d_τ is the separation of the partial under an applied stress. The first two terms relate to the energy required to bring the partials together and the last two terms refer to the energy required to recombine the cores.

Assuming $\Lambda = \frac{2Gb^2}{4\pi}$, as evaluated using non-linear elastic theory, and integrating gives,

$$E_R = \frac{3}{4} \frac{Ga^2}{24\pi} \cdot \left[\ln \left(\frac{d_\tau}{b} \right) - 1 \right] + \frac{G}{2\pi} (b^2 - b_1^2 - b_2^2) \tag{A5}$$

E_R is insensitive to changes in stress, since stress only affects the dislocation separation d_τ in the natural logarithm term.

6.3. W_{CS}, work done by local stress, resolved onto the cross-slip plane.

The dislocation, as a result of the local stress, bows in the cross-slip plane (csp) sweeping an area

$$\left[\frac{2\theta}{2\pi} (\pi r^2) - r^2 \sin\theta \cos\theta \right]$$

Hence,

$$W_{CS} = r^2(\theta - \sin\theta \cos\theta)\tau_{csp} b_{csp} \tag{A6}$$

6.4. ΔU_L, increase in dislocation line energy.

Considering Fig. 6c, it can be seen that the increase in line energy (ΔU_L) is given by,

$$\Delta U_L = (2r\theta - 2r \sin\theta)\Gamma_L \tag{A7}$$

7. Appendix II

Determination of θ_c

To form a stable dislocation loop, (Fig. 6) θ must

reach some critical value θ_c, such that when $\theta > \theta_c$, a decrease in energy is observed as θ increases (i.e. θ_c occurs when U_{CS} is a maximum).

Rewritting Equation 3 in terms of θ by using Equations A4, A6 and A7, differentiating and equating to zero for a maximum gives:

$$\frac{\partial U_{CS}}{\partial \theta} = 0 = 2r \cos\theta_c E_{R\,111} + 2r(1 - \cos\theta_c)\Gamma_{L\,100} + r^2(1 + \sin^2\theta_c - \cos^2\theta_c)(\gamma_{APB} - \tau b)_{100}$$

Hence

$$r\cos^2\theta_c(\tau b - \gamma_{APB})_{100} + \cos\theta_c(E_{R\,111} - \Gamma_{L\,100}) + (\Gamma_{L\,100} + r[\gamma_{APB} - \tau b]_{100}) = 0$$

Dividing by r and putting $\Gamma_{L\,100} = r(\tau b)_{100}$ gives,

$$\cos^2\theta_c(\tau b - \gamma_{APB})_{100} + \cos\theta_c \frac{(\tau b)_{100}}{\Gamma_{L\,100}} (E_{R\,111} - \Gamma_{L\,100}) + \gamma_{APB\,100} = 0$$

which on re-arranging yields,

$$\cos^2\theta_c(\tau b - \gamma_{APB})_{100} + \cos\theta_c(\tau b)_{100} \left[\frac{E_{R\,111}}{\Gamma_{L\,100}} - 1\right] + \gamma_{APB\,100} = 0$$

For Ni_3Al it can be shown that $E_{R\,111} \ll \Gamma_{L\,100}$ (typically 2 to 3%) [18], hence

$$\cos^2\theta_c(\tau b - \gamma_{APB})_{100} - \cos\theta_c(\tau b)_{100} + \gamma_{APB\,100} = 0$$

On solving for θ_c the following solutions are obtained

(i) $$\cos\theta_c = 1;\ \theta_c = 0$$

(ii) $$\cos\theta_c = \frac{\gamma_{APB\,100}}{(\tau b)_{100} - \gamma_{APB\,100}}$$

(ii) Acknowledgements

The authors would like to thank Professor J. G. Ball for the provision of research facilities. One of the authors (JRN) is indebted to the Science Research Council for a Research Studentship.

References

1. O. D. SHERBY and P. M. BURKE, *Prog. Mat. Sci.* **13** (7) (1967) 384.
2. P. H. THORNTON, R. G. DAVIES and T. L. JOHNSTON, *Met. Trans* **1** (1970) 207.
3. P. A. FLINN, *Trans. Met. Soc. AIME* **218** (1960) 145.
4. H. CONRAD, *Acta Met.* **6** (1958) 339.
5. J. WEERTMAN, *J. Appl. Phys.* **29** (1958) 1685.
6. A. SEEGER, "Dislocations and Mechanical Properties of Crystals" (Wiely , New York, 1957) p. 243.
7. G. SCHOECK and A. SEEGER, "Report on the Conference on Defects in a Crystalline Solid, (Phys. Soc., London, 1955) p. 340.
8. N. F. MOTT, "N.P.L. Creep and Fracture of Metals" (Philisophical Lib., New York, 1957) p. 21.
9. J. WEERTMAN, *J. Appl. Phys.* **26** (1955) 1213.
10. *Idem, ibid* **28** (1957) 362.
11. *Idem, ibid* **28** (1957) 1185.
12. A. H. COTTRELL, "Dislocations and Plastic Flow in Crystals" (Oxford U. P., London, 1953) p. 136.
13. F. R. N. NABARRO, Proceedings of the Conference of Strength of Solids, (Physical Soc., London, 1948) p. 75.
14. C. HERRING, *J. Appl. Phys.* **21** (1950) 437.
15. R. O. WILLIAMS; *Acta Met.* **5** (1957) 55.
16. R. L COBLE, *J. Appl. Phys.* **34** (1963) 1679.
17. J. R. NICHOLLS and R. D. RAWLINGS, *Acta Met.* **25** (1977) 187.
18. J. R. NICHOLLS, Ph.D. Thesis, Imperial College, London University (1974).
19. R. D. RAWLINGS and A. E. STATON-BEVAN, *J. Mater. Sci.* **10** (1975) 505.
20. A. E. STATON-BEVAN and R. D. RAWLINGS, *Phil. Mag.* **32** (1975) 787.
21. R. W. DICKSON, J. B. WATCHMAN and S. M. COPLEY, *J. Appl. Phys.* **40** (1969) 2276.
22. G. F. HANCOCK, *Phys. Stat. Sol. A* **7** (1971) 535.
23. N. JAFFE and J. E. DORN, *Trans. Met. Soc. AIME* **224** (1962) 1167.
24. A. E. STATON-BEVAN and R. W. RAWLINGS, *Phys. Stat. Sol. (a)* **29** (1975) 613.
25. A. N. STROH, *Proc. Roy Soc.* **A223** (1954) 404.
26. J. E. DORN, "Energetics in Metallurgical Phenomena", Vol. 1, edited by W. M. Mueller, (Gordon and Breach, London, 1964).

Received 28 February and accepted 4 Arpil 1977.